Available online at www.sciencedirect.com
SCIENCE DIRECT
Catalysis Today 107–108 (2005) 371–376
CATALYSIS TODAY
www.elsevier.com/locate/cattod

Influence of reducibility of vanadium–magnesium mixed oxides on the oxidative dehydrogenation of propane

L. Balderas-Tapia [a,b,*], I. Hernández-Pérez [b], P. Schacht [c], I.R. Córdova [a], G.G. Aguilar-Ríos [a]

[a] *Instituto Politécnico Nacional, Departamento de Ingeniería Química Industrial, ESIQIE, Av. IPN s/n, Edificio 7, 1er Piso, UPALM, 07738 México D.F., Mexico*
[b] *Universidad Autónoma Metropolitana-A, Área de Química Aplicada, Av. San Pablo 180, 02200 México D.F., Mexico*
[c] *Instituto Mexicano del Petróleo, Eje Central Lázaro Cárdenas 152, 07730 México D.F., Mexico*

Available online 22 August 2005

Abstract

A series of vanadium–magnesium mixed oxides used for the propane oxidative dehydrogenation were synthesized by combining the impregnation and precipitation methods. Several techniques such as, FTIR, XRD and TPR-H_2 were applied to characterize physicochemical properties. XRD analysis confirms that the V–Mg–O oxides consist of $Mg_3V_2O_8$ structure with VO_4 tetrahedral units together with periclase phase. Magnesium incorporation with vanadium inhibits the formation of V_2O_5 containing exposed V=O bonds. TPR-H_2 results show two peaks located between 500 and 750 °C, which, respectively, correspond to reduction of V^{5+} species in distorted VO_4 units and V^{5+} species belonging to bulk Mg orthovanadate. The highest activity and selectivity were obtained on catalysts in which isolated VO_4 tetrahedral are present. A relationship between reducibility degree of V^{5+} distorted species (into unities VO_4), and catalytic activity was observed. In order to get a higher activity a maximum content of 45% as vanadium oxide.

Keywords: Propane; Propene; Oxidative dehydrogenation; V-Mg-O catalysts; $Mg_3V_2O_8$; Reducibility

1. Introduction

Among the hydrocarbon oxidation processes, the oxidative dehydrogenation of light alkanes (C_2–C_6) provides a potential alternative route to alkenes; it is an exothermic reaction and the presence of O_2 in the reaction mixture inhibits carbon deposition [1,2]. Vanadium–magnesium oxides (V–Mg–O) have been proposed as catalysts for the oxidative dehydrogenation of *n*-butane [3–6], propane [7–13], cyclohexane [14] and ethylbenzene [15]. V-Mg-O mixed oxide catalysts are usually obtained by supporting vanadium oxide on MgO by conventional impregnation techniques, using an ammonium metavanadate solution [3,4,6,11]. Other preparation methods have also been employed, such as citrate methods [9], adsorption of vanadyl compounds from non-aqueous solutions [16], co-precipitation of Mg nitrate and NH_4VO_3 [17] or co-precipitation of Mg oxalate and vanadyl oxalate [10].

The phases of the Mg vanadates depend on the vanadium concentration and the preparation procedure, so the catalytic activity and selectivity of the catalysts are significantly affected by the preparation method [10,18,19]. In those reports, it has been proposed that VO_4 tetrahedral units are active sites of the oxidative dehydrogenation activity, at the same time the V=O double bonds mainly lead to deep oxidation products, i.e., CO_x. How to prepare active V-containing catalyst with more active species such as VO_4 tetrahedral units and how to inhibit the formation V=O bonds on the catalysts are a very interesting research topic. In this paper, we report a simple preparation method for obtaining V–Mg–O mixed oxides, containing a high content of VO_4 tetrahedral units, without double V=O bonds in order

* Corresponding author. Tel.: +52 55 5729 6000x55265; fax: +52 55 5586 2728.
E-mail address: lbalderast@ipn.mx (L. Balderas-Tapia).

0920-5861/$ – see front matter
doi:10.1016/j.cattod.2005.07.025

to improve the catalytic activity and to avoid deep oxidation competitive reactions.

2. Experimental

2.1. Preparation of V-Mg-O catalysts

$Mg(OH)_2$ was prepared by precipitation from a magnesium nitrate [$Mg(NO_3)_2{\cdot}6H_2O$, Aldrich, 99%] solution with ammonium hydroxide (NH_4OH, Baker) at pH = 9.0 and 50 °C under vigorous stirring conditions. Precipitate was aged for 24 h at room temperature, then washed repeatedly with demineralized water, filtrated and then dried overnight at 95 °C. MgO was prepared by calcinating of $Mg(OH)_2$ at 600 °C for 4 h. V_2O_5 was prepared from ammonium vanadate (NH_4VO_3, Aldrich, 99%) by thermal decomposition at 600 °C for 4 h in a stream of air. The temperature was raised with a rate at 2.8 °C/min. MgO and V_2O_5 were prepared to serve as a references. V-Mg-O catalysts were prepared as follows: an appropriate amount of $Mg(OH)_2$ powder was added to a basic hot aqueous solution containing ammonium metavanadate. The mixture was stirred for 1 h. The resulting suspension was evaporated to dryness at 85 °C followed by further drying at 95 °C for 12 h. The dried powders were crushed and calcined in air at 600 °C for 4 h.

2.2. Catalysts characterization

The chemical composition of the catalysts obtained was determined by atomic absorption spectroscopy (AAS) using a Perkin-Elmer 2380 apparatus.

Specific (BET) surface area, pore volume and pore size were determined from the corresponding nitrogen adsorption–desorption isotherm at 77 K using a Micromeritics ASAP 2000 apparatus.

X-ray diffraction (XRD) patterns were obtained with a Siemens D500 diffractometer equipped with a copper anode X-ray tube and a diffracted beam monochromator (Kα radiation).

Fourier transformed infrared (FTIR) spectra were recorded between 1200 and 400 cm^{-1} at room temperature with a Magna Nicolet 750 FTIR spectrometer. The samples were mixed with KBr (1/100 by weight) and pressed into a thin wafer.

Temperature-programmed reduction (TPR) was carried out in a Micromeritics TPD/TPR 2900 apparatus consisting of a quartz U-reactor using 10% H_2 in argon and a heating rate of 10 °C/min. The samples were pretreated in flowing N_2 (99.99%) at 450 °C for 0.5 h and cooled in N_2. During the reduction, samples were heated from 50 to 900 °C. The consumption of H_2 was measured using a thermal conductivity detector.

2.3. Catalytic test

The experiments were carried out at atmospheric pressure in a conventional fixed bed micro-reactor apparatus consisting of a mixing chamber, a glass reactor (U-type) and an on line gas chromatograph. The internal diameter of the reactor tube in the catalytic zone was 9 mm. The axial temperature profile was measured using a thermocouple placed in a thermowell centered in the catalyst bed. The total gas flow rate was 57.62 mL/min: the flow of propane was 10 mL/min and the flow air was 47.62 mL/min. The catalyst loading was 0.15 g with a particle size of 0.147–0.175 mm. Experiments were performed at 460 °C. Prior testing the catalyst was pretreated in situ with air at 460 °C for 1 h. The products were analyzed by on-line gas chromatography. The chromatograph used was a Perkin-Elmer autosystem XL equipped with a TC detector.

3. Results and discussion

The chemical composition, specific surface area, pore volume and pore size of the catalysts are presented in Table 1. Specific areas result increased by incorporating of vanadium oxide into MgO. Particularly, the catalyst containing 15 wt.% of vanadium oxide, the specific surface area had a two-fold increase. However, as the vanadium oxide content raised (15–45 wt.%), both, the specific area and the pore volume gradually decreased. Pure MgO sample showed a tri-modal pore size distribution: a small amount at 35 Å and two main peaks centered approximately at 88 and 246 Å. As the vanadium content increased in the V–Mg–O mixed samples, more pores with a maximum diameter of about 30 Å were developed, as indicated by the growth of this peak. However, the number of pores with a size around 90 Å gradually diminished and finally disappeared when the vanadium oxide content was 60 wt.%. Based on these

Table 1
Textural properties of V–Mg–O oxides calcined at 600 °C for 4 h

Samples	Composition		Specific area (m^2/g)	Pore volume (cm^3/g)	Pore diameter, average (Å)		
	MgO (wt.%)	V_2O_5 (wt.%)			Pore 1	Pore 2	Pore 3
MgO	100	0	66.7	0.29	35	88	246
15VMgO	84.9	14.8	122.1	0.27	30	65	306
30VMgO	69.9	29.9	89.0	0.25	35	114	295
45VMgO	54.8	44.8	68.8	0.16	30	242	

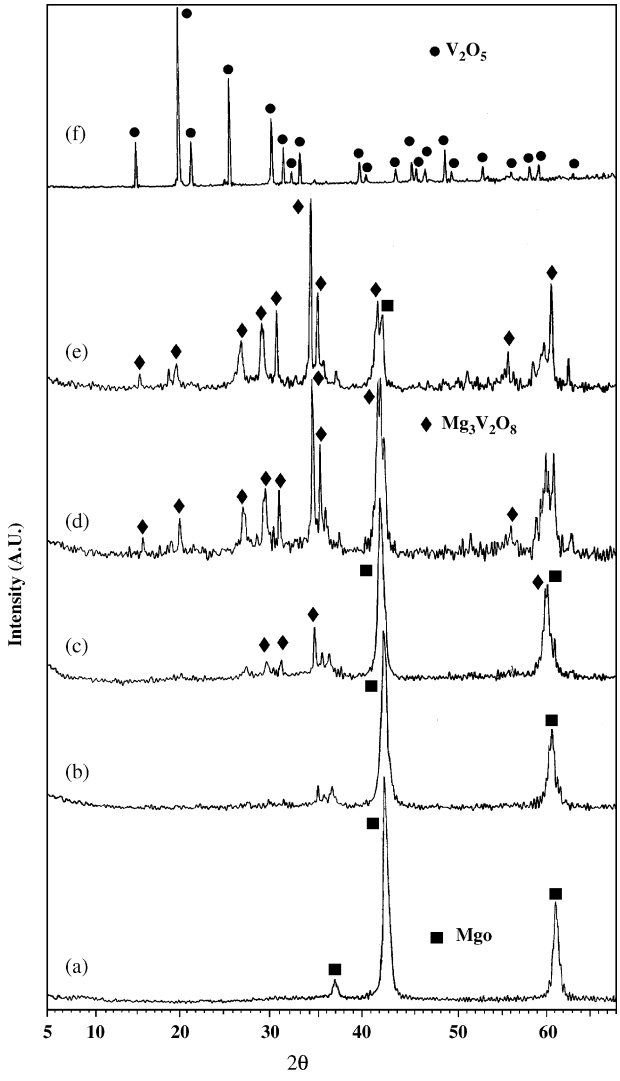

Fig. 1. XRD patterns of V–Mg–O materials calcined at 600 °C for 4 h: (a) MgO; (b) 15VMgO; (c) 30VMgO; (d) 45VMgO; (e) 60VMgO; (f) V_2O_5.

results, it possible to conclude that the textural properties of the V-Mg-O catalysts are very sensitive to the chemical composition and the pore diameter distribution can be controlled by varying the V/Mg ratio in the preparation stage.

Fig. 1 shows the XRD patterns of the magnesium oxides, vanadium oxide and mixed V–Mg–O samples. The XRD diffractrogram of the magnesium oxide were indexed as periclase (MgO), and vanadium oxide was identified as vanadium pentoxide (V_2O_5). Each sample in the V–Mg–O oxides consists of two crystallographic phases of Mg orthovanadate ($Mg_3V_2O_8$) and magnesium oxide (MgO). Neither pyrovanadate ($Mg_2V_2O_7$) nor metavanadate (MgV_2O_6) were detected. Furthermore, the vanadium oxide (V_2O_5) was not formed in the V–Mg–O samples. For 15VMgO sample, enriched in Mg, MgO was the major phase. However, as the vanadium oxide content was higher than 30 wt.%, the main diffraction peaks are associated to the contribution of Mg orthovanadate phase. The formation of the Mg orthovanadate phase is very important, because it has been proved that vanadium (V^{5+}) cations in tetrahedral oxo-coordination $Mg_3V_2O_8$ are the active phase for the oxidative dehydrogenation of alkanes [9,10,19]. Since the alkane molecule is activated and adsorbed on the reactive surface oxygen from the isolated tetrahedral VO_4 units, they remove an H atom from the hydrocarbon molecule to form an adsorbed propyl radical and a surface OH group, this greatly favours the catalytic activity and the selectivity to alkenes [10,20].

The infrared spectra of the V_2O_5, MgO and V–Mg–O samples in the region 400–1200 cm^{-1} are shown in Fig. 2. In these spectra the contribution from MgO was not subtracted. The bands that appeared at 1019, 826, 600 and 485 cm^{-1} are characteristic for bulk V_2O_5. The spectrum of 60VMgO consisted of bands at 917, 859, 830, 691 and 456 cm^{-1}. All of these bands correspond to the vibrations of Mg orthovanadate phase [11,20]. Bands that appeared at 859 cm^{-1} due to the ν_3 antisymmetric stretch of $(VO_4)^{3-}$

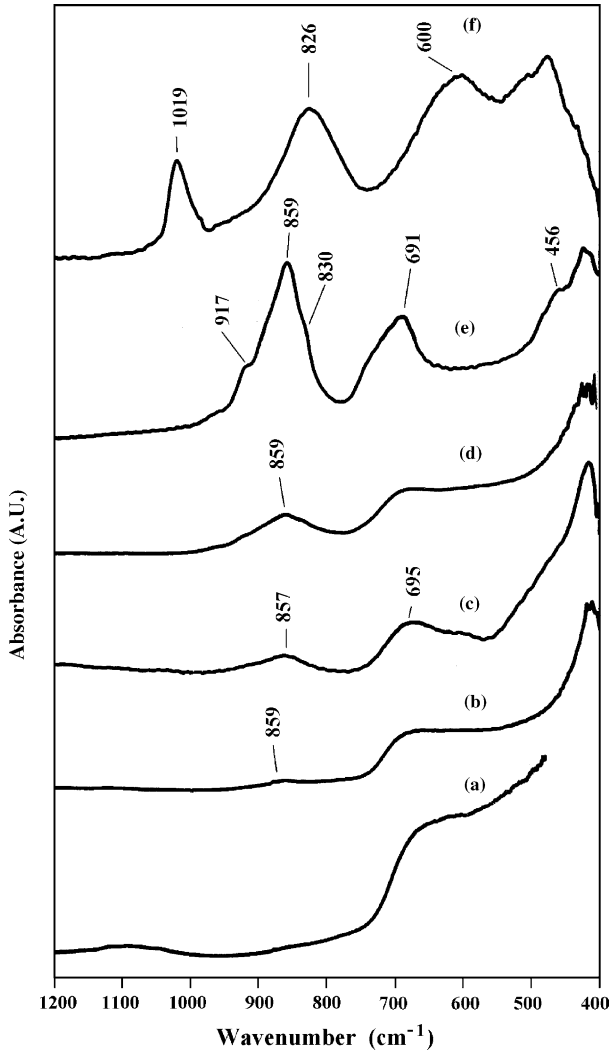

Fig. 2. Infrared spectra of V–Mg–O mixed oxides calcined at 600 °C for 4 h: (a) MgO; (b) 15VMgO; (c) 30VMgO; (d) 45VMgO; (e) 60VMgO; (f) V_2O_5.

anions, whereas the bands 691 and 456 cm^{-1} are characteristic of ν_{as} and ν_s of V–O–V bond, respectively [11]. It is well established that V_2O_5 forms a layer structure on TiO_2 (anatase) and alumina to expose the (0 1 0) plane preferentially. There is a high density of V=O groups on this (0 1 0) plane. The V=O groups possess a characteristic infrared stretching frequency at 1020 cm^{-1}[20,21]. As shown in Fig. 2, this characteristic V=O stretching was not observed in the V–Mg–O samples. The FTIR analysis confirms well the results by XRD analysis. Based on XRD and FTIR results, we infer that the incorporating of magnesium oxide into the vanadium oxide effectively inhibits the formation of V_2O_5 with V=O bonds, where V^{5+} are in octahedral coordination, usually shows a poor selectivity to olefins during the oxidative dehydrogenation of alkanes, due to the double V=O bonds resulting from incorporation of oxygen in the intermediate reaction products, thus leading to formation of oxygenate compounds [22–24]. Therefore, the elimination of the V_2O_5 phase in the V–Mg–O oxides is in favour of enhancing the catalytic selectivity to olefins. The presence of isolated VO_4 tetrahedral species and the absence of V=O double bonds in the V–Mg–O are the significant differences between the supported or pure vanadate and our V–Mg–O mixed oxides. These differences make possible to use the V–Mg–O mixed as catalysts in the oxidative dehydrogenation of propane.

Fig. 3 shows the TPR-H_2 profiles of the V_2O_5 and MgO and V–Mg–O samples. The TPR plots of the V_2O_5 sample showed two peaks located at 700 and 737 °C which are associated to the following reduction steps [25]:

$$V_2O_5 \rightarrow \tfrac{1}{3}V_6O_{13} \rightarrow V_2O_4$$

In the V–Mg–O mixed oxides, there are two peaks in range from 450 to 750 °C. According to Blasco et al., the low-temperature peaks can be assigned to the reduction of isolated V^{5+} species in distorted VO_4 tetrahedral environments on the catalyst surface, whereas the high-temperature peaks correspond to the reduction of V^{5+} species from the bulk structure of Mg orthovanadate ($Mg_3V_2O_8$) [26,27], the reduction of the oxygen species in distorted VO_4 units is relatively easy compared to the V_2O_5. As the vanadium content increased, the peak at low temperature gradually grew in area, however, the one at high temperature progressively reduce its area and finally disappeared. The temperatures corresponding to the peak maximum (T_{ml} and T_{mh}) in TPR profiles and their corresponding shifts are reported in Table 2. It is noted that the T_{ml} of the lower temperature peak were shifted from 600 to 618, 682 and 712 °C when the vanadium oxide content increased from 15 to 30, 45 and 60 wt.%, respectively, concerning to 15VMgO, its high-temperature peak, T_{mh}, shifted 39 °C for the 30VMgO sample and 68 °C for 45VMgO towards a higher temperature range. These shifts of peak temperatures indicate that the reduction of the corresponding oxygen species becomes difficult in the samples with high vanadium content.

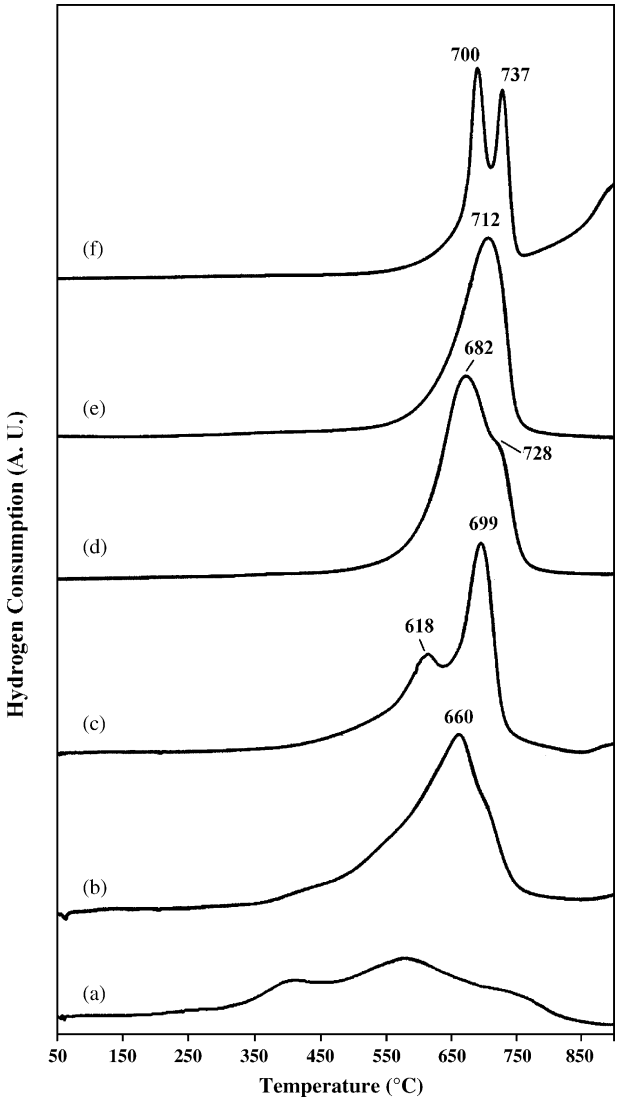

Fig. 3. Temperature-programmed reduction plots of V–Mg–O mixed oxides: (a) MgO; (b) 15VMgO; (c) 30VMgO; (d)45VMgO; (e) 60VMgO; (f) V_2O_5.

The results of the catalysts tests of V-Mg-O catalysts at 460 °C are presented in Table 3, in which selectivity concern the formation of propene. Oxidative dehydrogenation and combustion are the major reactions. V_2O_5 is active, but its

Table 2
TPR results of the V–Mg–O samples

Samples	T_{ml} (°C)	ΔT_{ml} (°C)	T_{mh} (°C)	ΔT_{mh} (°C)
15VMgO	600		660	
30VMgO	618	18	699	39
45VMgO	682	82	728	68
60VMgO	712	112		

T_{ml}: temperature corresponding to the peak maximum of the peak at lower temperature; T_{mh}: temperature corresponding to the peak maximum of the peak at higher temperature; ΔT_{ml}: T_{ml} difference between the samples and 15VMgO; ΔT_{mh}: T_{mh} difference between the samples and 15VMgO.

Table 3
Catalytic performance of the V-Mg-O catalysts

Catalyst	Conversion, C_3H_8 (%)	Selectivity		Stability (3 h/1 h)
		C_3H_6 (%)	CO_x (%)	
MgO				
15VMgO	5.37	28.4	71.6	87.6
30VMgO	6.60	26.6	73.4	87.4
45VMgO	7.12	23.1	76.9	89.1
60VMgO	5.48	30.7	69.3	95.8
V_2O_5	3.5	15.3	89.7	89.9

Reaction conditions: catalyst, 0.15 g; C_3H_8 flow rate, 10 mL/min; air flow rate, 47.62 mL/min; temperature, 460 °C.

selectivity for propene is low. MgO is neither active nor selectivity. All the V-Mg-O catalysts are more active than the simples oxides. Depending on the vanadium oxide content on the catalysts, differences in total activity as well as in selectivity to propene were obtained. Partially oxygenated products were not observed on any catalyst. The influence of the vanadium oxide content on the propane conversion and propene selectivity is given in Fig. 4. From these data, it can be concluded that the maximum activity is obtained on the 45VMgO catalyst. In Fig. 5, it is presented the influence of the propane conversion on the selectivity to propene, at 460 °C, on different V-Mg-O catalysts. It can be seen that 60VMgO has the best selectivity for propene, 15VMgO is in the middle, 45VMgO is worst.

Table 4 summarizes the literature data about the effect of phase composition on the catalytic performance. All these catalysts have a good selectivity to propene at low conversions, but increasing the conversion (by increasing the temperature and/or the residence time) decreases the selectivity to the olefin; thereupon the results obtained at different conditions, cannot be consistently correlated. In our case, the highest catalytic activity is obtained with catalysts with low vanadium oxide content. In this case, one can expect to have isolated VO_4 tetrahedron on the catalysts surface. However, it is possible that on V-Mg-O catalysts the formation of tetrahedral vanadium species occurs also at higher vanadium content.

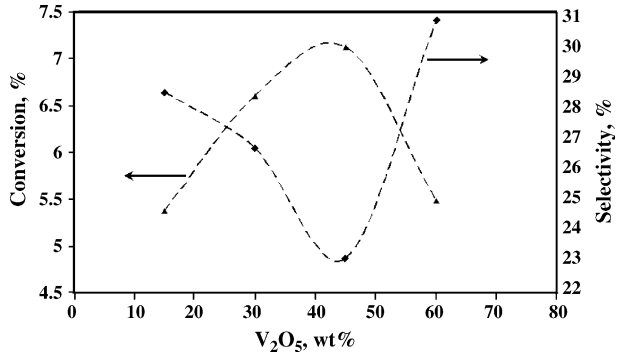

Fig. 4. Influence of the catalysts vanadium content (wt.% of V_2O_5) on the propane conversion and propene selectivity, obtained at 460 °C.

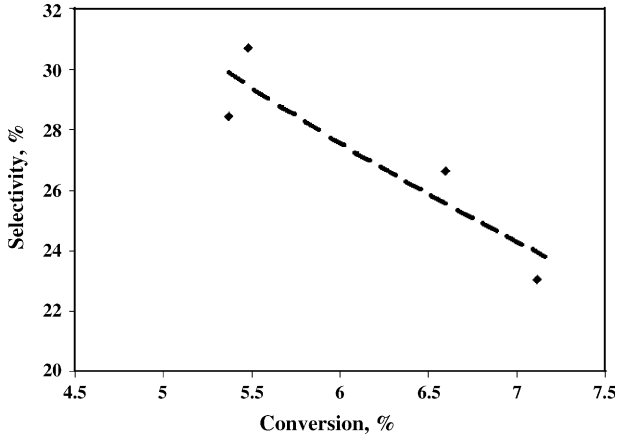

Fig. 5. Propane selectivity as a function of propane conversion. Catalytic conditions: $T = 460$ °C; $C_3H_6/O_2 = 1$; total flow rate = 57.62 mL/min; catalysts weight = 0.15 g.

In addition, we must indicate that the TPR-H_2 results, obtained for the V-Mg-O catalysts, show two peaks associated to two different vanadium species [26,27]. From the comparison between TPR-H_2 data and the catalytic results, it has been concluded that a parallelism between catalytic activity and reducibility occurs. In this way, the insolated VO_4 tetrahedra present a greater reducibility than the Mg orthovanadate (6OVMgO).

Finally, the catalytic properties of V-Mg-O catalysts for the oxidative dehydrogenation of propane are affected by the reducibility of the oxygen species on the catalysts. The vanadium content in the V–Mg–O system should be limited

Table 4
Performance of V-Mg-O catalysts in the oxidative dehydrogenation of propane as a function of phase composition

Phase composition	*X* (%)	*S* (%)
A		
MgO	34	23
MgO, $Mg_2V_2O_7$	33	30
MgO, $Mg_3V_2O_8$, $Mg_2V_2O_7$	18	40
$Mg_2V_2O_7$, $Mg_3V_2O_8$ > MgO	10	42
B		
MgO, $Mg_3V_2O_8$	43	34.5
MgO, $Mg_3V_2O_8$	25.9	52.4
$Mg_3V_2O_8$	24	46.6
C		
MgV_2O_6	13.1	46.5
$Mg_2V_2O_7$	14.9	50.0
$Mg_3V_2O_8$	3.9	58.3
D		
MgO		
MgO > $Mg_3V_2O_8$	5.37	28.4
MgO > $Mg_3V_2O_8$	6.6	26.6
MgO, $Mg_3V_2O_8$	7.12	23.1
$Mg_3V_2O_8$ > MgO	5.48	30.7

(A) Reaction temperature = 500 °C; $C_3H_8/O_2 = 0.1$ [11]. (B) Reaction temperature = 500 °C; $C_3H_8/O_2 = 0.5$ [9]. (C) Reaction temperature = 450 °C; $C_3H_8/O_2 = 3.5$ [28]. (D) Reaction temperature = 460 °C; $C_3H_8/O_2 = 1.0$ [this work].

in a reasonable range, i.e., in our case, no more than 45 wt.%.

4. Conclusions

A simple preparation method to obtain vanadium–magnesium mixed oxides with mesoporous structure for propane oxidative dehydrogenation has been reported. Varying the V/Mg ratio, it is possible to obtain the V–Mg–O biphasic samples with a bimodal or trimodal pore size distribution. XRD and FTIR characterization show that the formation of the vanadium pentoxide phase with octahedral V^{5+} in double V=O bonds, was completely inhibited in the Mg–V–O mixed oxides prepared with our method. The selectivity to propene is a function of the conversion of propane. The $Mg_3V_2O_8$ phase containing isolated VO_4 tetrahedral species with greater reducibility was formed, which favours the enhancement of the catalytic activity of propane oxidative dehydrogenation.

Acknowledgement

L. Balderas-Tapia would like to thank the financial support from CONACyT (Mexico), for his doctoral study at the Universidad Autónoma Metropolitana-Azcapotzalco, Mexico.

References

[1] F. Cavani, F. Trifiró, Catal. Today 51 (1999) 561.
[2] T. Blasco, J.M. López Nieto, Appl. Catal. A 157 (1997) 117.
[3] A.A. Lemonidou, Appl. Catal. A 216 (2001) 277.
[4] C. Tellez, M. Abon, J.A. Dalmon, C. Mirodatos, J. Santamaría, J. Catal. 195 (2000) 113.
[5] J.M. López-Nieto, A. Dejoz, M.I. Vazquez, W.O. Leary, J. Cunningham, Catal. Today 40 (1998) 215.
[6] M.A. Chaar, D. Patel, M.C. Kung, H.H. Kung, J. Catal. 105 (1987) 483.
[7] A. Pantazidis, A. Burrows, C.J. Kiely, C. Mirodatos, J. Catal. 177 (1998) 325.
[8] S.R.G. Carrazán, C. Peres, J.P. Bernard, M. Ruwet, P. Ruiz, B. Delmon, J. Catal. 158 (1996) 452.
[9] X. Gao, P. Ruiz, Q. Xin, X. Guo, B. Delmon, J. Catal. 148 (1994) 56.
[10] A. Corma, J.M. López Nieto, N. Paredes, J. Catal. 144 (1993) 425.
[11] D.S.H. Sam, V. Soenen, J.C. Volta, J. Catal. 123 (1990) 417.
[12] M.C. Kung, H.H. Kung, J. Catal. 128 (1991) 287.
[13] L. Late, E.A. Blekkan, J. Nat. Gas Chem. 11 (2002) 33.
[14] J. Hanuza, B. Jezowaska-Trzebiatowska, W. Oganowski, J. Mol. Catal. 29 (1985) 109.
[15] J. Kijenski, A. Baiker, M. Glinsky, P. Dollenmeier, A. Wokaun, J. Catal. 101 (1986) 1.
[16] V.K. Sharma, A. Wokaum, A. Baiker, J. Phys. Chem. 90 (1986) 2715.
[17] M. Del Arco, M.J. Holgado, C. Martín, V. Rives, J. Mater. Sci. Lett. 6 (1987) 616.
[18] A. Corma, J.M. López Nieto, N. Paredes, M. Perez, Appl. Catal. 97 (1993) 159.
[19] M.C. Kung, H.H. Kung, J. Catal. 134 (1992) 668.
[20] M.A. Chaar, D. Patel, M.C. Kung, H.H. Kung, J. Catal. 105 (1987) 483.
[21] A. Miyamoto, Y. Yamazaki, M. Inomata, Y. Murakami, J. Phys. Chem. 85 (1981) 2366.
[22] G. Buaca, Catal. Today 27 (1996) 465.
[23] S.T. Oyama, J. Catal. 128 (1991) 210.
[24] H.H. Kung, Adv. Catal. 40 (1994) 1.
[25] H. Bosch, B.J. Kip, J.G. van Ommen, P.J. Gellings, J. Chem. Soc. Faraday Trans. 1 80 (1984) 2479.
[26] T. Blasco, J.M. López-Nieto, A. Dejoz, M.I. Vázquez, J. Catal. 157 (1995) 271.
[27] A. Corma, J.M. López-Nieto, N. Paredes, A. Dejoz, M.I. Vázquez, in: V. Cortés Corberán, S. Vic Bellón (Eds.), New Developments in Selective Oxidation II, Elsevier, Amsterdam, Stud. Surf. Sci. Catal. 82 (1994) 113.
[28] S. Sugiyama, T. Hashimoto, N. Shigemoto, H. Hayashi, Catal. Lett. 89 (2003) 229.